BIOCHEMISTRY
including biophysical chemistry & molecular biology

Article

pubs.acs.org/biochemistry

Activation of the Epidermal Growth Factor Receptor: A Series of Twists and Turns

David Poger*,† and Alan E. Mark†,‡

†School of Chemistry and Molecular Biosciences, The University of Queensland, Brisbane, QLD 4072, Australia
‡Institute for Molecular Bioscience, The University of Queensland, Brisbane, QLD 4072, Australia

ABSTRACT: The cell surface epidermal growth factor receptor (EGFR) plays a critical role in cell development and oncogenesis. The binding of growth factors to the EGFR results in a mechanical signal being transmitted through the plasma membrane. In this study, atomistic molecular dynamics simulations have been used to investigate the conformational changes associated with the binding of the epidermal growth factor (EGF) and transforming growth factor α (TGFα) to the EGFR. In the simulations, the removal of the EGF and TGFα from the extracellular domain of the EGFR homodimer led to a relative rotation of the protomers of 16−35° about the dimerization axis. The three N-terminal domains that make up the extracellular region of the receptor undergo essentially rigid-body motion. The dimerization interface itself was found to be largely unaffected by the removal of the ligand. In most simulations, the rotation within the dimer was associated with an opening of the cytokine-binding sites. On the basis of these simulations, a simple mechanical model that explains the coupling between the binding of ligand and the motions in the extracellular domains is proposed.

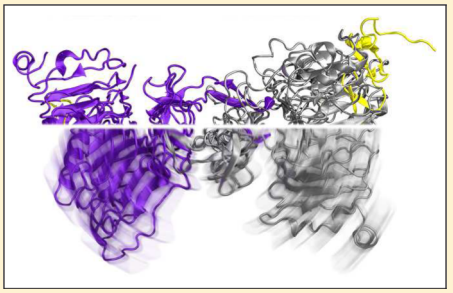

Understanding the mechanism by which the binding of a growth factor to its receptor induces the transmission of a signal across the plasma membrane is quite important in cell regulation. While it has long been accepted that receptor activation results from the dimerization of receptor molecules subsequent to ligand binding,[1,2] studies of various cytokine receptors now suggest that dimerization alone is not sufficient for activation. Instead, conformational rearrangements within the protomers are now considered to play a critical role.[2,3]

Receptor tyrosine kinases (RTKs) are membrane-spanning cytokine receptors, the intracellular domain of which possesses an intrinsic kinase activity. The epidermal growth factor receptor (EGFR, also known as ErbB1 or HER1) is the prototypical member of the EGFR family of RTKs. The EGFR family also includes ErbB2 (Neu/HER2), ErbB3 (HER3), and ErbB4 (HER4). ErbB receptors modulate key stages in the development of organisms, such as cell proliferation, motility, differentiation, and tissue homeostasis. Enhancement of their activity promotes tumorigenesis.[4−6] A wide range of related peptide growth factors [including the epidermal growth factor (EGF), transforming growth factor α (TGFα), amphiregulin, betacellulin, epigen, epiregulin, heparin-binding EGF-like growth factor, and neuregulins (or heregulins)] are known to interact with members of the ErbB receptor family. All these peptides except neuregulins can bind to the EGFR, but only EGF, TGFα, amphiregulin, and epigen associate specifically with the EGFR homodimer.[7] To date, only structures of a soluble form of the human EGFR (termed sEGFR) homodimer bound to EGF[8,9] and TGFα[10] have been determined in atomic detail. Like all RTKs, the EGFR consists of a ligand-binding extracellular domain connected to an intracellular domain by a single-pass, transmembrane α-helix. ErbB receptors can associate into homo- or heterodimers.[4] Panels A and B of Figure 1 show the structure of the homodimer of the extracellular domain of the human EGFR (residues 1−621). The extracellular domain of each protomer contains four subdomains: domain I (residues 1−165), domain II (residues 166−309), domain III (residues 310−481), and domain IV (residues 482−621; truncated in Figure 1A,B), alternatively termed leucine-rich domain 1 (L1), cysteine-rich domain 1 (CR1), L2, and CR2, respectively.[11,12] Domains I and III fold as a β-helix or solenoid structure and together form the cytokine-binding site. Domains II and IV are organized into a series of small, laminin-like disulfide-bonded modules. These modules contain either a single disulfide bond or two intertwined disulfide bonds. Domains II and IV are composed of eight and seven modules, respectively. In the crystal structures of the EGFR dimer, the two domains II interact along the 2-fold axis of symmetry. The closest interactions are found between two large β-hairpins ("dimerization arms") that protrude from each domain II and make contact with the other domain II.[8,10,13]

Historically, the EGFR has been considered the archetypical RTK. Nevertheless, the activation mechanism of the EGFR differs from those of other RTKs in terms of its mode of dimerization and the conformational rearrangements that are thought to accompany activation. Crystal structures of the extracellular domain of several growth factor receptors such as the fibroblast growth factor receptor (FGFR)[14] and the stem

Received: December 6, 2013
Revised: April 3, 2014
Published: April 4, 2014

dx.doi.org/10.1021/bi401632z | *Biochemistry* 2014, 53, 2710−2721

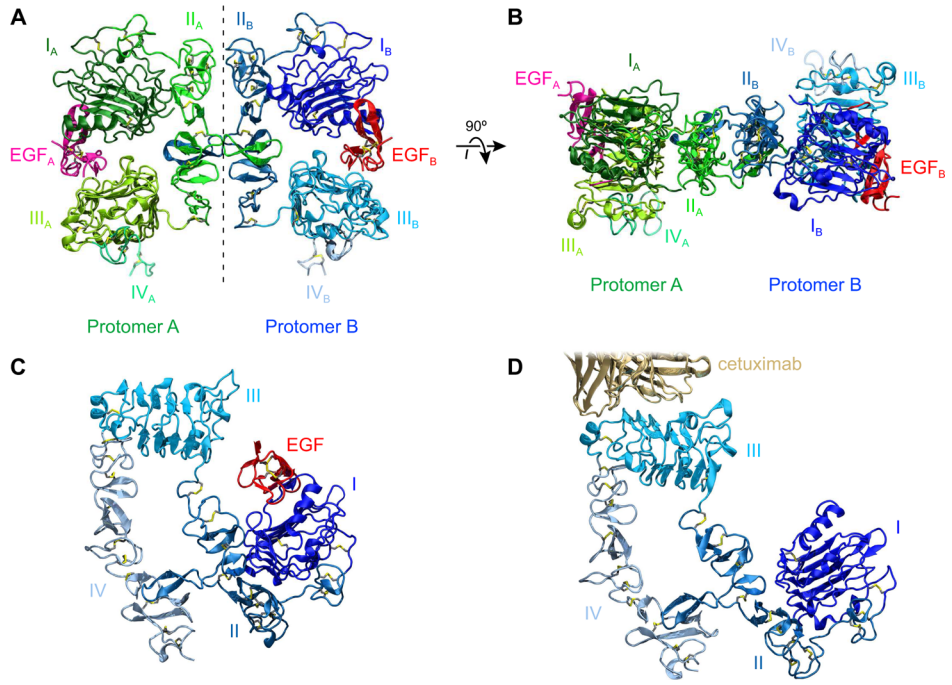

Figure 1. Structure of the EGFR extracellular domain in the active (A and B) and autoinhibited (C and D) states. (A) View of the structure of the EGF-bound homodimer of the soluble EGFR extracellular domain (sEGFR).[8] The 2-fold symmetry axis is oriented vertically and indicated by a dashed line. The two protomers are denoted with subscripts A and B. Domains I–III and truncated domain IV in protomers A and B are shown in shades of green and blue, respectively. The two molecules of the EGF bound to protomers A (EGF_A) and B (EGF_B) are colored magenta and red, respectively. The structure of the TGFα-bound homodimer is similar.[10] (B) Top view of the EGF-bound sEGFR homodimer looking down toward the plasma membrane. (C) Structure of the EGF-bound autoinhibited configuration of the EGFR extracellular domain.[23] (D) Structure of the inactive complex of the EGFR extracellular domain stabilized by the antigen-binding fragment of the antibody cetuximab.[24] Cetuximab is colored beige. For the sake of clarity, the structure of the antigen-binding fragment of cetuximab is truncated.

cell factor receptor (KIT),[15,16] suggest that the ligand may facilitate receptor dimerization by binding at the dimerization interface with only small changes in the structure of the protomers themselves. In contrast, the crystal structures of the dimeric form of the soluble extracellular domain of the EGFR (sEGFR) bound to EGF[8,9] and TGFα[10] show the formation of a back-to-back dimer mediated exclusively by interactions between domain II of each protomer. The two cytokines in the complex are bound to only one of the sEGFR molecules and lie on opposite sides of the dimer. They do not contribute directly to the dimerization interface (Figure 1A,B). In addition, whereas the dimerization of receptors appears to occur only after ligand binding in the case of other RTKs, ErbB receptors have been shown to reversibly self-associate in the absence of ligand, forming a pool of inactive dimers on the cell surface.[17−22] Crystal structures of the monomeric EGFR obtained in the presence and absence of a ligand (panels C and D of Figure 1, respectively)[23,24] suggest that activation may be associated with substantial conformational rearrangements within each receptor molecule. In the unliganded, monomeric structure, the dimerization arm of domain II interacts with the membrane-proximal domain IV, forming a compact auto-inhibited structure. However, in the presence of a ligand (EGF or TGFα), the extracellular domain in the dimer adopts an extended conformation.[25,26]

Although these structures provide considerable insight into how the binding of growth factors affects the conformation of the extracellular domain, the fundamental mechanistic question of how ligand binding leads to the transmission of a mechanical signal into the cytosol remains largely unexplored. To date, molecular dynamics simulation studies of the EGFR have mainly focused on the structure of the cytokine-bound extracellular domain of the EGFR in monomeric and homodimeric states in solution, in a crystal environment, or in the presence of a membrane.[27−30] Nuclear magnetic resonance spectroscopy, mutagenesis, and simulation studies have shown that ligand binding alters the structure of the transmembrane domain and promotes the dimerization of an N-terminal motif located in the first two turns of the transmembrane α-helix.[9,31,32] The rotation or twisting of the juxtamembrane regions in the EGFR following EGF binding has also been proposed.[17,33] However, how this motion might be coupled to any conformational change within the EGFR has not been elucidated in detail. In this study, molecular dynamics simulations have been used to investigate the nature of the structural rearrangement within the sEGFR homodimer that occur upon EGF or TGFα binding. The simulations suggest that the domains undergo a rigid-body motion between the two receptor molecules. This torsional motion appears to be coupled to the opening of the cytokine-binding sites.

METHODS

System Setup. The coordinates of the holo sEGFR complexes were taken from the crystal structures of the EGF-bound[8] and TGFα-bound[10] sEGFR dimer [Protein Data Bank (PDB) entries 1ivo and 1mox, respectively]. The residues and atoms for which no density was observed in the $(sEGFR–EGF)_2$ dimer (protomer A, L1; protomer B, L1 and E2; EGF A and B, N1–S4, L52, and R53) and the $(sEGFR–TGF\alpha)_2$ dimer (protomer A, L1, E2, K202, D290, E295, V299–K301, K303, E306, P308, R310, K311, and S501; protomer B, L1, E2, K202,

dx.doi.org/10.1021/bi401632z | Biochemistry 2014, 53, 2710−2721

D290, E296, V299, K301, K303, K304, E306, and P308; TGFα A, V1, V2, and S11; TGFα B, V1, V2, and S11−T13) were constructed using PyMOL.[34] In both crystal structures, domain IV in each protomer was truncated (after V512 and S501 in PDB entries 1ivo and 1mox, respectively). The missing amino acids in domains IV were not modeled. Instead, the C-terminus of each protomer was capped with a neutral amido group. Note, in 2010, the structure of $(sEGFR{-}EGF)_2$ was re-refined, including domain IV.[9] However, to compare the effects of the two ligands, the EGF and TGFα, directly, the truncated form of the sEGFR (without domain IV) was used in all simulations. The structure of the sEGFR apo dimer was derived from the two crystal structures of holo dimers $(sEGFR{-}EGF)_2$ and $(sEGFR{-}TGF\alpha)_2$ by removing the cytokines (apo dimers denoted $sEGFR^E{}_2$ and $sEGFR^T{}_2$, respectively).

Each system (holo and apo homodimers) was hydrated and energy-minimized. The temperature of each system was then gradually increased from 50 to 298 K in 50 K steps over 120 ps to further relax the system and obtain the starting configurations used in the later work.

Simulation Parameters. All simulations of the unliganded, EGR-bound, and TGFα-bound forms of the soluble, truncated EGFR extracellular domain (termed sEGFR) were performed using GROMACS version 3.3.3[35] in conjunction with the GROMOS 54A7 force field.[36] Each system was simulated under periodic conditions in a truncated octahedral box with explicit water. The temperature of the system was maintained by independently coupling the protein and water to an external temperature bath at 298 K with a coupling constant of 0.1 ps using a Berendsen thermostat.[37] The pressure was maintained at 1 bar by weakly coupling the system to an isotropic pressure bath[37] using an isothermal compressibility of 4.6×10^{-5} bar^{-1} and a coupling constant of 1 ps. Covalent bond lengths within the protein were constrained using the Lincs algorithm.[38] The geometry of the simple point charge (SPC) water molecules[39] was constrained using Settle.[40] The hydrogen atoms in the protein were replaced by virtual interaction sites. Their positions were constructed at each step from the coordinates of the heavy atoms to which they are attached.[41] This allowed a 4 fs time step to be used without affecting the thermodynamic properties of the system significantly. Nonbonded interactions were evaluated using a twin-range cutoff scheme: interactions falling within the 0.8 nm short-range cutoff were calculated every step, whereas interactions within the 1.4 nm long-range cutoff were updated every two steps, together with the pair list. A reaction-field correction was applied to the electrostatic interactions beyond the long-range cutoff[42] using a relative dielectric permittivity constant of 62, as appropriate for SPC water.[43] The two systems consisting of the homodimeric extracellular domain of the EGFR in the holo state bound to either two EGF or two TGFα molecules were each simulated four times for 40 ns [simulations $HE_1{-}HE_4$ for $(sEGFR{-}EGF)_2$ and simulations $HT_1{-}HT_4$ for $(sEGFR{-}TGF\alpha)_2$]. The simulations of the unliganded $(sEGFR)_2$ homodimers were conducted four times each for 65 or 100 ns (simulations $AE_1{-}AE_4$ for $sEGFR^E{}_2$ and simulations $AT_1{-}AT_4$ for $sEGFR^T{}_2$). An overview of the simulations performed is given in Table 1.

Analysis. *Root-Mean-Square Deviation.* The root-mean-square deviation (rmsd) of the coordinates of the backbone atoms (N, Cα, C, and O) with respect to a reference structure was calculated after performing a least-squares fit of the backbone atoms to the reference structure.

Table 1. Overview of the Systems Simulated

system	simulation	initial PDB structure	simulation time (ns)
holo dimer			
$(sEGFR{-}EGF)_2$	HE_1	1ivo	40
	HE_2	1ivo	40
	HE_3	1ivo	40
	HE_4	1ivo	40
$(sEGFR{-}TGF\alpha)_2$	HT_1	1mox	40
	HT_2	1mox	40
	HT_3	1mox	40
	HT_4	1mox	40
apo dimer			
$sEGFR^E{}_2$	AE_1	1ivo	100
	AE_2	1ivo	100
	AE_3	1ivo	65
	AE_4	1ivo	65
$sEGFR^T{}_2$	AT_1	1mox	100
	AT_2	1mox	100
	AT_3	1mox	65
	AT_4	1mox	65

Twist Angle within the Dimer. Twist angle Ω within the apo and holo dimers was defined as the angle between an axis joining the two centers of mass of the two domains I and an axis joining the two centers of mass of the two domains III in the sEGFR dimer. A schematic representation of Ω is shown in Figure 2B.

Torsion Angle within Each Protomer. To calculate the torsion angle between domains I and III along the long axis of domain II in each protomer, domain II was split into two subdomains of 72 residues: N-terminal subdomain II_1 (residues 166−237) and C-terminal subdomain II_2 (residues 238−309). Torsion angles ϕ_A and ϕ_B in protomers A and B, respectively, were calculated as the dihedral angle between a plane defined by the centers of mass of domain I and subdomains II_1 and II_2 for ϕ_A and a plane defined by the centers of mass of subdomains II_1 and II_2 and domain III for ϕ_B. A schematic representation of ϕ_A and ϕ_B is given in Figure 2C.

Opening of the Ligand-Binding Site in Each Protomer. The extent to which the ligand-binding site in each protomer was closed or opened was quantified as follows. The opening of the ligand-binding pocket in a given protomer was estimated from angle θ (θ_A and θ_B in protomers A and B, respectively) defined by the center of mass of the three following groups of atoms: domain I of the protomer, the cluster formed by the two dimerization arms (residues 239−269 in domain II of each protomer), and domain III of the same protomer (Figure 2D).

Distances between the Two Domains III and IV in the Dimer. Distances d_{III} and d_{IV} were defined as the distances between the centers of mass of the two domains III (III_A and III_B) and IV (IV_A and IV_B), respectively (Figure 2E).

Contact Surface Area. Contact surface area C between two molecules m and n was estimated as

$$C = \frac{1}{2}(A_m + A_n - A_{mn}) \quad (1)$$

where A_m, A_n, and A_{mn} are the solvent-accessible surface areas of molecule m alone, molecule n alone, and the complex formed by molecules m and n, respectively. The solvent-accessible surface area was calculated using the method of Lee and Richards[44] with a probe radius of 0.14 nm as implemented in

dx.doi.org/10.1021/bi401632z | Biochemistry 2014, 53, 2710−2721

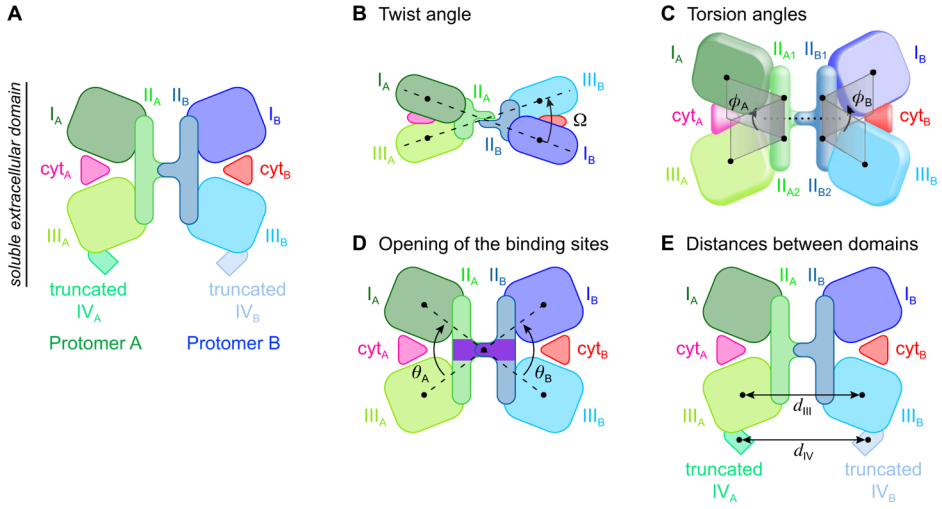

Figure 2. Schematic view of the motions calculated from the simulations. (A) Schematic representation of the soluble extracellular domain (sEGFR). The two cytokines are denoted cyt_A and cyt_B. (B) Top view of the sEGFR representing twist angle Ω within the dimer. The centers of mass of domains I_A, III_A, I_B, and III_B are denoted with black dots. (C) Torsion angles ϕ_A and ϕ_B within the protomers. Subdomains 1 and 2 in each domain II are separated by a dotted line. The centers of mass of domains I_A, III_A, I_B, and III_B and subdomains II_{A1}, II_{A2}, II_{B1}, and II_{B2} are denoted with black dots. (D) Opening angles θ_A and θ_B of the ligand-binding sites in the protomers. The cluster formed by the two modules 5 in domains II_A and II_B is colored purple. The centers of mass of domains I_A, III_A, I_B, and III_B and the cluster of the two modules 5 are denoted with black dots. (E) Distances d_{III} and d_{IV} between the centers of mass of the two domains III and the two truncated domains IV, respectively. The centers of mass of domains III_A and III_B and truncated domains IV_A and IV_B are denoted with black dots.

VMD.[45,46] The contact surface area was calculated for the interface between the cytokines and the sEGFR dimer (C_c) and for the dimerization interface between the two protomers of the sEGFR dimer (C_d).

RESULTS

Stability of the Structure of the sEGFR Dimer. To investigate the structural stability of the homodimer of the soluble extracellular domain of the EGFR (sEGFR) bound to either two EGF or two TGFα molecules, four independent simulations for each complex starting from their respective X-ray structures [PDB entries 1ivo for $(sEGFR–EGF)_2$[8] and 1mox for $(sEGFR–TGF\alpha)_2$[10]] were performed, leading to eight simulations in total.

To examine whether the structure of the two sEGFR molecules within the dimer was maintained during the simulations, the root-mean-square deviation (rmsd) of the positions of the backbone atoms of each sEGFR with respect to the initial corresponding crystal structure was calculated. The rmsds were averaged over the last 10 ns of each simulation. The overall structure of the receptor molecules was stable in all the simulations. On average, the rmsd was 0.49 ± 0.07 nm for $(sEGFR–EGF)_2$ and 0.47 ± 0.07 nm for $(sEGFR–TGF\alpha)_2$ and did not depend on the nature of the cytokine present. Note that while a rmsd of 0.5 nm for a single-domain protein may be considered significant, the sEGFR is a large multidomain protein and the overall rmsd is due to small changes in the relative positions of the individual domains. The structure of these domains (I_A, II_A, and III_A and I_B, II_B, and III_B) was essentially retained in all the simulations. Note that subscripts A and B refer to the two sEGFR protomers. The integrity of domains IV_A and IV_B was not analyzed in detail as significant proportions of these domains were missing in both initial PDB structures. The rmsds calculated ranged from 0.17 to 0.43 nm. Interestingly, the lowest rmsd value was obtained for domains I_A and I_B in all eight simulations (0.18 ± 0.04 nm). The largest rmsds were obtained for the two domains II (0.40 ± 0.10 and 0.32 ± 0.08 nm for domains II and III, respectively). Domain II is composed of multiple modules, and the higher rmsds result from changes in the relative positions of the modules. No difference was found between systems $(sEGFR–EGF)_2$ and $(sEGFR–TGF\alpha)_2$. The cytokines were stable in all simulations. The average rmsd calculated with respect to the initial crystal structure was 0.26 ± 0.04 nm for the EGF in $(sEGFR–EGF)_2$ and 0.25 ± 0.07 nm for TGFα in $(sEGFR–TGF\alpha)_2$.

The removal of the two EGF molecules from $(sEGFR–EGF)_2$ and the two TGFα molecules from $(sEGFR–TGF\alpha)_2$ led to a change in the relative orientation of the domains in each sEGFR protomer. Note that the two apo homodimers are denoted $sEGFR^E_2$ and $sEGFR^T_2$, respectively. The change in the relative orientation of the protomers is associated with an increase in the average rmsd of each protomer with respect to the starting crystal structure, that is 1.02 ± 0.12 nm for $sEGFR^E_2$ and 0.74 ± 0.21 nm for $sEGFR^T_2$. The average rmsd values were calculated after the systems had equilibrated for 30 ns (i.e., 30–100 ns for simulations AE_1, AE_2, AT_1, and AT_2 and 30–65 ns for simulations AE_3, AE_4, AT_3, and AT_4). The length of time over which the averages were computed did not affect the final values significantly. This demonstrates that the systems had reached a quasi equilibrium within 30 ns. Interestingly, the variation in the backbone rmsd is larger in the simulations of $sEGFR^E_2$ than in those of $sEGFR^T_2$. The effect of the removal of the cytokine differed among the three domains in each protomer but was comparable in magnitude in all of the apo systems. The average rmsd values for each domain were 0.24 ± 0.04 nm (domain I), 0.63 ± 0.11 nm (domain II), and 0.42 ± 0.04 nm (domain III) in the simulations of $sEGFR^E_2$ and 0.20 ± 0.03 nm (domain I), 0.56 ± 0.10 nm (domain II), and 0.45 ± 0.09 nm (domain III) in the simulations of $sEGFR^T_2$. The conformational changes in both protomers were similar. The magnitudes were greater in domain II than in domains I and III. Again, domain I had the lowest rmsd. Nonetheless, a comparison of the final structures from the apo and holo simulations yielded rmsd values of 0.26, 0.40, and 0.43 nm on

dx.doi.org/10.1021/bi401632z | Biochemistry 2014, 53, 2710–2721

Table 2. Twist, Rotation, and Cytokine-Binding Site Opening Angles and Interdomain Distances in the Apo and Holo sEGFR Dimers[a]

system	Ω (°)	ϕ_A (°)	ϕ_B (°)	θ_A (°)	θ_B (°)	d_{III} (nm)	d_{IV} (nm)
holo dimer							
$(sEGFR–EGF)_2$	29.3 (4.7)	23.1 (5.6)	19.2 (2.8)	63.4 (1.7)	62.4 (1.4)	6.3 (0.2)	7.9 (0.4)
1ivo	*14.5*	*9.3*	*11.2*	*56.7*	*56.7*	*6.8*	*7.7*
$(sEGFR–TGF\alpha)_2$	8.6 (3.6)	19.1 (6.1)	16.1 (5.8)	60.7 (2.2)	60.6 (1.0)	6.4 (0.4)	8.5 (0.9)
1mox	*2.2*	*2.7*	*6.1*	*55.8*	*55.4*	*6.7*	*7.6*
apo dimer							
$sEGFR^E_2$	64.7 (3.0)	61.5 (2.8)	63.6 (1.7)	73.4 (6.8)	75.1 (6.9)	6.7 (0.3)	7.3 (0.7)
$sEGFR^T_2$	24.9 (8.7)	32.9 (1.9)	40.5 (1.3)	55.9 (11.3)	55.3 (8.0)	7.1 (0.2)	8.1 (0.7)

[a]A schematic description of the motions is shown in Figure 2. θ_A and θ_B are the opening angles of the cytokine-binding site in protomers A and B, respectively (Figure 2D). ϕ_A and ϕ_B are the torsional angles in protomers A and B, respectively (Figure 2C). Ω is the twist angle of the dimer (Figure 2B). d_{III} and d_{IV} are distances between the two domains III and IV, respectively (Figure 2E). The values of the angles and distances in the crystal structures of the EGF- and TGFα-bound dimers (PDB entries 1ivo and 1mox, respectively[10,8]) are shown in italics. The numbers in parentheses are the standard deviations of the averages calculated over four simulations.

average for domains I–III, respectively, between the simulations of $(sEGFR–TGF\alpha)_2$ and $sEGFR^T_2$ and 0.27, 0.47, and 0.48 nm for domains I–III, respectively, between the simulations of $(sEGFR–EGF)_2$ and $sEGFR^E_2$. This suggests that the nature of the relaxation of each of the domains in the protomers was similar in all cases and independent of the specific cytokine in the original crystal structure.

Relative Orientation of the sEGFR Protomers within the Receptor Dimer. In the crystal structures of the dimers containing the two alternative cytokines, the two protomers lie at an angle with respect to each other. In $(sEGFR–EGF)_2$, twist angle Ω (illustrated in Figure 2B) is 14.5°, whereas in $(sEGFR–TGF\alpha)_2$, Ω is 2.2°. Although the structures of the individual protomers were largely conserved during the simulations of $(sEGFR–EGF)_2$ and $(sEGFR–TGF\alpha)_2$, the relative orientation of the protomers varied compared to the starting X-ray structures. In all simulations, the relaxation of the holo dimers involved a rotation about the C_2 axis of the complex (i.e., along the long axis of the dimer formed by domains II_A and II_B). This occurred within the first 10–15 ns. Over the last 10 ns of the simulation, Ω was 29.3 ± 4.7° and 8.6 ± 3.6° in $(sEGFR–EGF)_2$ and $(sEGFR–TGF\alpha)_2$, respectively. The values of the rotation angles calculated from the simulations are listed in Table 2. The time evolution of Ω in simulations HE_1 of $(sEGFR–EGF)_2$ and HT_1 of $(sEGFR–TGF\alpha)_2$ is illustrated in Figure 3. Note, by convention, a twist angle is positive if, looking down the C_2 symmetry axis (i.e., toward the plasma membrane), the rotation is counterclockwise.

The twist in the dimer is due to the protomers undergoing an internal rotation about the long axis of each domain II whereby the position of domain I moves in a counterclockwise direction with respect to domain III. The two protomers within the dimer experience comparable motions with the values of the torsion angles calculated (ϕ_A in protomer A and ϕ_B in protomer B, illustrated in Figure 2C) being similar: ϕ_A = 23.1 ± 5.6° and ϕ_B = 19.2 ± 2.8° in $(sEGFR–EGF)_2$, and ϕ_A = 19.1 ± 6.1° and ϕ_B = 16.1 ± 5.8° in $(sEGFR–TGF\alpha)_2$. The values of ϕ_A and ϕ_B calculated from the simulations and the crystal structures are listed in Table 2.

The removal of the two EGF or TGFα molecules induced a further twist in the dimers within 20–30 ns. The extent of the rotation was different in the two apo systems: Ω = 64.7 ± 3.0° for $sEGFR^E_2$, and Ω = 24.9 ± 8.7° for $sEGFR^T_2$ (from 30 ns onward). Note that, after the initial relaxation, the new

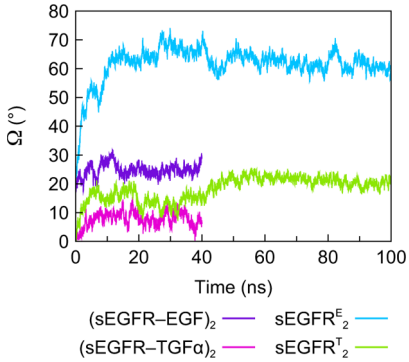

Figure 3. Time evolution of twist angle Ω in the holo dimers $(sEGFR–EGF)_2$ and $(sEGFR–TGF\alpha)_2$ and apo dimers $sEGFR^E_2$ and $sEGFR^T_2$ in simulations HE_1, HT_1, AE_1, and AT_1, respectively.

orientation of the protomers in the unliganded state was stable. No dissociation of the dimer or additional rotation was observed within 100 ns (simulations AE_1, AE_2, AT_1, and AT_2) or 65 ns (simulations AE_3, AE_4, AT_3, and AT_4). For example, Figure 3 shows that Ω plateaus after approximately 40–50 ns in the simulations of the apo dimer. The final structures of $(sEGFR–EGF)_2$ in simulation HE_1 and $sEGFR^E_2$ in simulation AE_1 are shown in Figure 4. Both structures are superimposed onto the initial crystal structure (colored gray). It is clear that despite the magnitude of the rotation in $sEGFR^E_2$, the dimer retained its 2-fold symmetry along the long axis of the dimerization interface.

The overall change in the relative orientation of the protomers in the apo dimer stemmed from a twist within each protomer that occurred within the first 20–30 ns. This is illustrated in Figure 5 using simulations HE_1 and AE_1 for $(sEGFR–EGF)_2$ and $sEGFR^E_2$, respectively, in panel A and simulations HT_1 and AT_1 for $(sEGFR–TGF\alpha)_2$ and $sEGFR^T_2$, respectively, in panel B. As one can see, there is little change in the values of ϕ_A and ϕ_B in the simulation of the liganded dimers (HE_1 and HT_1). In contrast, there is a dramatic increase in the torsional angle in the case of the apo dimers after removal of the cytokines (simulations AE_1 and AT_1). In all simulations, the magnitude of torsion angle ϕ was similar for the two protomers (ϕ_A = 61.5 ± 2.8° and ϕ_B = 63.6 ± 1.7° in $sEGFR^E_2$, and ϕ_A = 32.9 ± 1.9° and ϕ_B = 40.5 ± 1.3° in $sEGFR^T_2$), indicating that the changes involved a concerted motion. Unlike the simulations of $sEGFR^E_2$, those of $sEGFR^T_2$ displayed significant variations in the magnitude of the torsion

dx.doi.org/10.1021/bi401632z | Biochemistry 2014, 53, 2710–2721

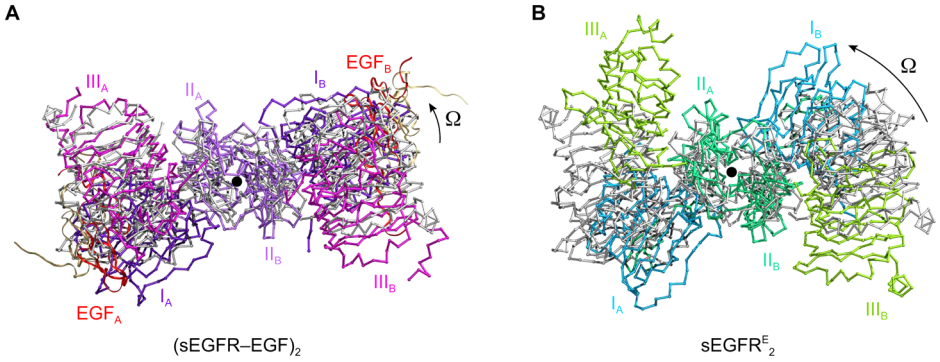

Figure 4. Top view of the structures of the twisted sEGFR dimer at the end of the simulations. (A) Superimposition of domains I–III of the crystal structure of $(sEGFR–EGF)_2$ with the final structure of a simulation of $(sEGFR–EGF)_2$ (simulation HE_1). The 2-fold symmetry axis represented by the black dot is oriented vertically toward the cell. The crystal structure is colored gray. Domains I–III in the two protomers in the structure from simulation HE_1 are colored purple, violet, and magenta, respectively. The EGF is colored beige and red in the crystal and simulation structures, respectively. (B) Superimposition of domains I–III of the crystal structure of $(sEGFR–EGF)_2$ with the final structure of a simulation of apo dimer $sEGFR^E_2$ (simulation AE_1). The crystal structure is colored gray. Domains I–III in the two protomers in the structure from simulation AE_1 are colored blue, dark green, and light green, respectively. The arrows indicate the direction of twist angle Ω. The structures were fit on the basis of the backbone atoms of domains II_A and II_B.

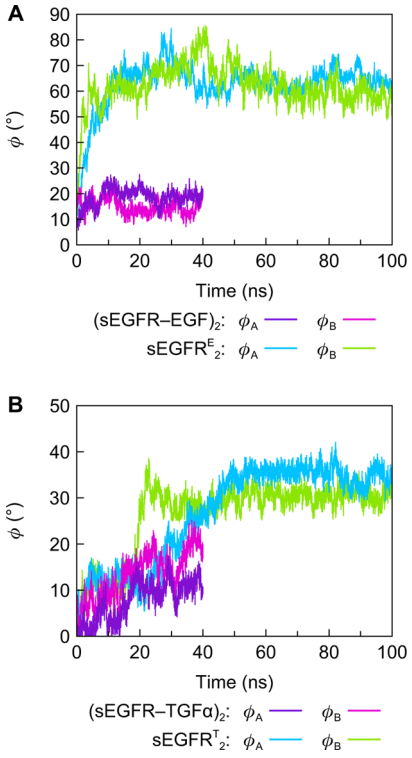

Figure 5. Rotation within the protomers of the sEGFR dimer. (A) Time evolution of torsional angles ϕ_A and ϕ_B in protomers A and B, respectively, in simulations of the holo $(sEGFR–EGF)_2$ (simulation HE_1) and apo $sEGFR^E_2$ (simulation AE_1) dimers. (B) Time evolution of torsional angles ϕ_A and ϕ_B in protomers A and B, respectively, in simulations of the holo $(sEGFR–TGF\alpha)_2$ (simulation HT_1) and apo $sEGFR^T_2$ (simulation AT_1) dimers.

angle. Nonetheless, ϕ_A and ϕ_B remained constant after the initial relaxation period as shown in Figure 5. Figure 6 shows a side view (i.e., perpendicular to the C_2 axis of the dimer) of protomer A at the end of simulations HE_1, AE_1, HT_1, and AT_1 of $(sEGFR–EGF)_2$, $sEGFR^E_2$, $(sEGFR–TGF\alpha)_2$, and $sEGFR^T_2$, respectively. Despite differences in the extent of motion and the orientation of domain III_A between the structures derived from the EGF- and TGFα-bound crystal structures, the relative arrangements of domains I_A, II_A, and III_A in the liganded forms are similar.

The distances between the two C-terminal domains in each sEGFR molecule were largely unaffected by the removal of the cytokines. Distances d_{III} and d_{IV} between domains III_A and III_B and between domains IV_A and IV_B, respectively, are listed in Table 2. In the crystal structures, d_{III} = 6.7–6.8 nm and d_{IV} = 7.6–7.7 nm. In the simulations, on average, $d_{III} \approx$ 6.4 nm and $d_{IV} \approx$ 8.2 nm in $(sEGFR–EGF)_2$ and $(sEGFR–TGF\alpha)_2$ and $d_{III} \approx$ 6.9 nm and $d_{IV} \approx$ 7.7 nm in apo dimers $sEGFR^E_2$ and $sEGFR^T_2$.

Configuration of the Ligand-Binding Sites. In all simulations of the unliganded and liganded sEGFR dimers, the change in the relative positions of the domains within the protomers was associated with a change in the opening of the cytokine-binding sites. The degree of opening was quantified by angles θ_A and θ_B in protomers A and B, respectively (illustrated in Figure 2D). The values of θ_A and θ_B are listed in Table 2. In the two crystal structures, the angle of the opening of the cytokine-binding sites was approximately 55–57°. In the simulations of the liganded dimers, the values of θ_A and θ_B were comparable: approximately 61–63° in both $(sEGFR–EGF)_2$ and $(sEGFR–TGF\alpha)_2$. Interfacial contact surface area C_c between the EGF or TGFα and the sEGFR dimer was also virtually unchanged with respect to those in the crystal structures [14.5 nm^2 in $(sEGFR–EGF)_2$[8] and 15.3 nm^2 in $(sEGFR–TGF\alpha)_2$[10]], with approximately one-third of the total solvent-accessible surface area of the cytokine buried by interactions with the receptor molecules: C_c = 15.9 ± 1.4 nm^2 for EGF in the simulations of $(sEGFR–EGF)_2$, and C_c = 13.8 ± 1.0 nm^2 for TGFα in the simulations of $(sEGFR–TGF\alpha)_2$.

In the simulations of the apo dimer, there were differences between the $sEGFR^E_2$ and $sEGFR^T_2$ complexes. After the removal of the EGF from $(sEGFR–EGF)_2$, the binding sites opened (θ_A = 73.4 ± 6.8°, and θ_B = 75.1 ± 6.9°), whereas the removal of TGFα from the TGFα-bound-derived dimer had in general little effect on the opening angle (θ_A = 55.9 ± 11.3°, and θ_B = 55.3 ± 8.0°). The exception was simulation AT_2 of $sEGFR^T_2$ in which the final angle was similar to that in the simulations of $sEGFR^E_2$ (θ_A = 74.8 ± 3.2°, and θ_B = 68.1 ± 1.2°). Note that the extent of opening or closure of the two

dx.doi.org/10.1021/bi401632z | Biochemistry 2014, 53, 2710–2721

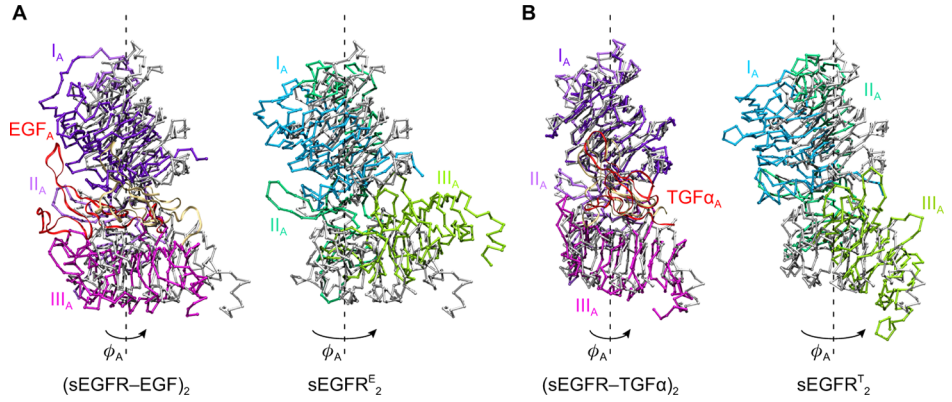

Figure 6. Side views of the structures of protomer A at the end of the simulations. (A) Superimposition of domains I–III of the crystal structure of (sEGFR–EGF)$_2$ with the final structure of simulations of (sEGFR–EGF)$_2$ (simulation HE$_1$, left) and sEGFR$^E_2$ (simulation AE$_1$, right). (B) Superimposition of domains I–III of the crystal structure of (sEGFR–TGFα)$_2$ with the final structure of simulations of (sEGFR–TGFα)$_2$ (simulation HT$_1$, left) and sEGFR$^T_2$ (simulation AT$_1$, right). In the crystal structures, the sEGFR and the cytokine (EGF or TGFα) are colored gray and beige, respectively. In the structures from the simulations, domains I–III are colored purple, violet, and magenta, respectively, in the holo sEGFR and blue, dark green, and light green, respectively, in the apo sEGFR. The cytokine is colored red. The arrows indicate the direction of the rotation. The structures were fit on the basis of the backbone atoms of domains II_A.

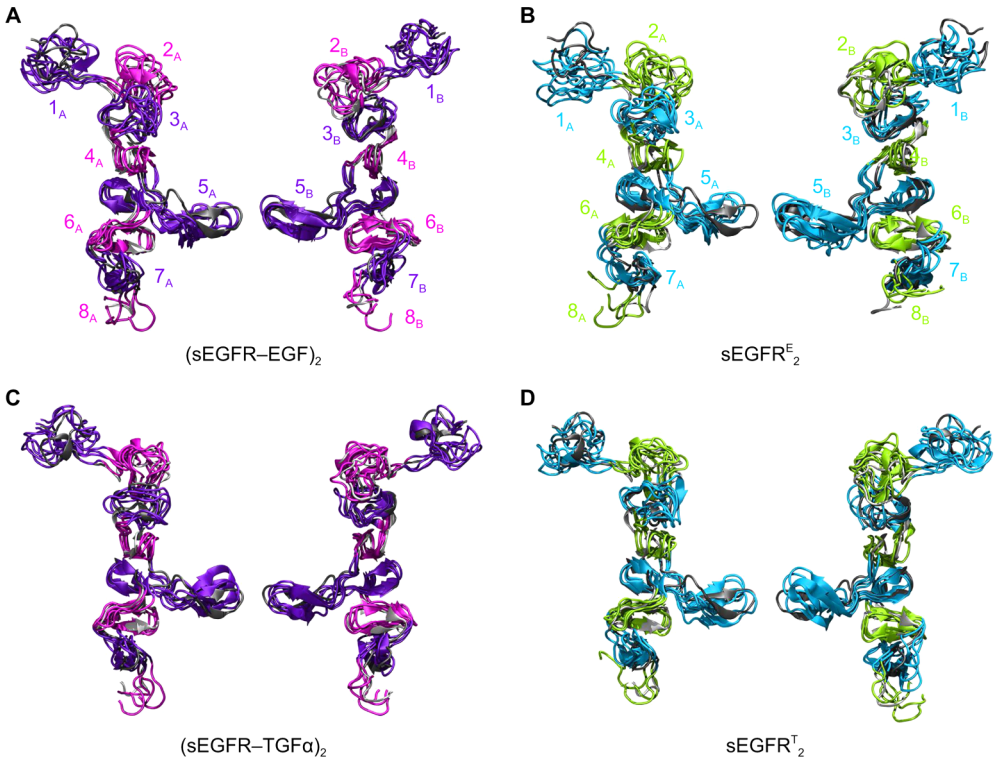

Figure 7. Superimposition of the crystal structure and the final structures of domains II_A and II_B in the sEGFR dimer from the simulations of (A) (sEGFR–EGF)$_2$, (B) sEGFR$^E_2$, (C) (sEGFR–TGFα)$_2$, and (D) sEGFR$^T_2$. In each panel, domain II_A is on left and domain II_B on the right. The modules in domains II_A and II_B in the starting crystal structures are colored dark gray and light gray, those in the holo dimers purple and magenta (panels A and C), and those in the apo dimers blue and green (panels B and D), respectively. The names of the modules are given in panels A and C. The structures were fit on the basis of the backbone atoms of each domain.

binding sites was similar in all the simulations, which strongly suggests that the binding sites are tightly coupled.

Structure and Dynamics of the Dimerization Interface. Given that domain II plays a central role in defining the interprotomer twist axis, the structural rearrangements with domain II as well as within the dimerization interface were examined in detail. As noted earlier, domain II undergoes the largest changes upon cytokine removal (average backbone rmsd of 0.63 ± 0.11 nm in sEGFR$^E_2$ and 0.56 ± 0.10 nm in sEGFR$^T_2$). Domain II consists of eight modules (residues 166–186, 187–207, 208–225, 226–238, 239–269, 270–285, 286–304, and 305–309). Figure 7 shows a superimposition of the final structures of domains II_A and II_B in all the simulations of the unliganded and liganded dimers with respect to their initial crystal structure (the modules are depicted in alternating colors). The variation in the rmsd calculated over the backbone atoms of each of the eight modules in domains II_A and II_B from 30 ns onward in all the simulations with respect to the initial

dx.doi.org/10.1021/bi401632z | *Biochemistry* 2014, 53, 2710–2721

crystal structures is plotted in Figure 8. From Figures 7 and 8, it can be seen that despite domain II showing the largest rmsd

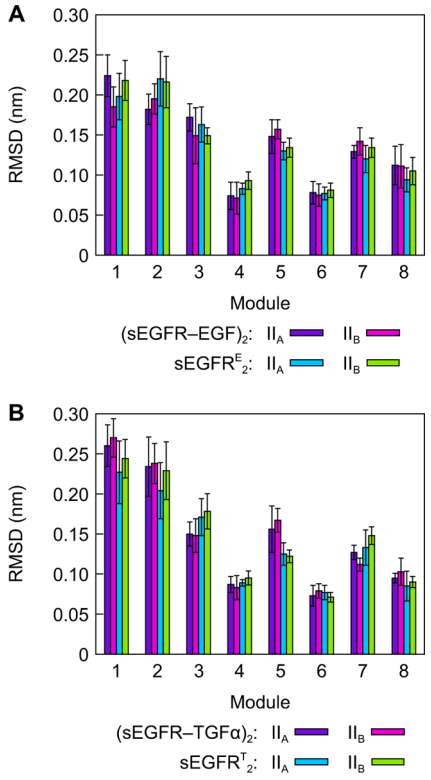

Figure 8. Variations in the structure of the modules in domains II_A and II_B in the holo and apo sEGFR dimers in the simulations derived from the crystal structures of (A) $(sEGFR–EGF)_2$ and (B) $(sEGFR–TGF\alpha)_2$. The structures were fit on the basis of the backbone atoms of all modules.

values, the overall conformational changes that occurred in the simulations were small, regardless of whether a cytokine was present. Furthermore, no significant difference was observed between the simulations derived from the two crystal structures. However, some of the eight modules did undergo internal structural changes. The flexibility decreases from modules 1 and 2 [rmsds of approximately 0.18–0.22 nm in $(sEGFR–EGFR)_2$ and $sEGFR^E_2$ and 0.23–0.26 nm in in $(sEGFR–TGF\alpha)_2$ and $sEGFR^T_2$] to module 8 (rmsd of approximately 0.08–0.10 nm in all the simulations and both protomers). The largest variations in the rmsd values between the simulations were found for modules 1 and 2 with standard deviations of approximately 0.04–0.08 nm. Interestingly, modules 4 and 6 that flank the dimerization arms have the lowest rmsds in all cases (0.08 nm on average).

The dimerization interface involves only domain II in the two crystal structures. The contact surface area of the dimerization interface was estimated to be 12.2 and 10.4 nm^2 per monomer in the crystal structures of $(sEGFR–EGF)_2$ and $(sEGFR–TGF\alpha)_2$, respectively. In all the simulations, the contact surface area was on average 20–50% larger [15.9 ± 0.7, 15.5 ± 0.7, 15.1 ± 0.6, and 14.6 ± 0.7 nm^2 in $(sEGFR–EGFR)_2$, $(sEGFR–TGF\alpha)_2$, $sEGFR^E_2$, and $sEGFR^T_2$, respectively]. Figure 9 shows average contact surface area C_d between each of the eight modules of domain II in a protomer and the whole domain II of the other protomer in the two crystal structures and the simulations [panel A, $(sEGFR–EGFR)_2$ and

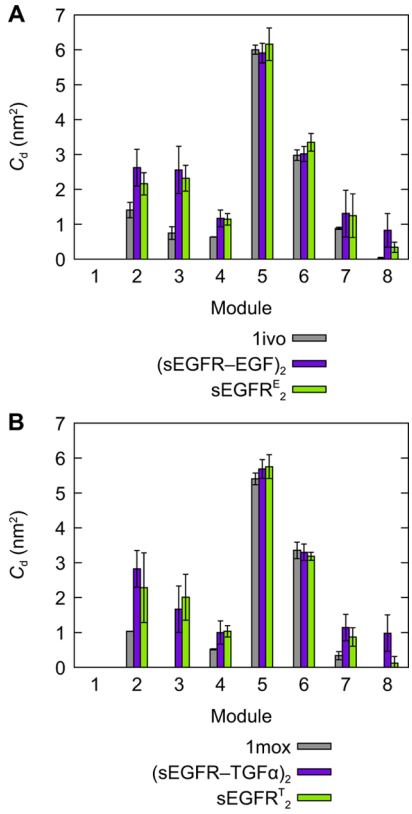

Figure 9. Variations in contact surface area C_d between each of the modules in domain II of one protomer and domain II of the other protomer in the holo (purple) and apo (green) sEGFR dimers in the simulations with respect to the starting crystal structures (gray). (A) $(sEGFR–EGF)_2$ and $sEGFR^E_2$. (B) $(sEGFR–TGF\alpha)_2$ and $sEGFR^T_2$.

$sEGFR^E_2$; panel B, $(sEGFR–TGF\alpha)_2$ and $sEGFR^T_2$]. Overall, the contacts in the simulations were similar in the unliganded and liganded dimers. Notable differences between the crystal structures and the simulations occur in modules 2–4 and 8 for which C_d is doubled in the simulations. In particular, modules 3 and 8 that did not participate significantly in the dimerization interface in the two crysral structures do contribute in all simulations. The most striking example is for module 3, for which the contact surface area reaches approximately 2.6, 1.7, 2.4, and 2 nm^2 in $(sEGFR–EGFR)_2$, $(sEGFR–TGF\alpha)_2$, $sEGFR^E_2$, and $sEGFR^T_2$, respectively. Of all the modules, the extent of contacts in the dimerization interface is greatest in modules 5 and 6 and, importantly, is unchanged when going from the crystal structure to the liganded and unliganded forms in the simulations ($C_d \approx 5.7$ nm^2 for module 5, and $C_d \approx 3.1$ nm^2 for module 6). No interprotomer contacts involving module 1 were found in any simulation, in line with the crystal structures.

Comparison with Inhibited Structures. Two structures of the inactive, monomeric, extracellular domain of the EGFR wherein domain II interacts with domain IV have been determined: the autoinhibited structure [PDB entry 1nql (Figure 1C)][23] and the inhibited structure in complex with the antigen-binding fragment from the antibody cetuximab [PDB entry 1yy9 (Figure 1D)].[24] For comparison, the rmsd of the backbone atoms of each sEGFR (domains I–III) of the unliganded and liganded dimers extracted from the simulations was calculated with respect to these two crystal structures. As expected, the conformational rearrangement associated with

dx.doi.org/10.1021/bi401632z | Biochemistry 2014, 53, 2710–2721

domain II contacting domain IV leads to large differences with both the unliganded and liganded dimers (rmsd > 1.7 nm). However, upon superimposition of domains I–III individually, rmsds are much lower (rmsd ≤ 0.52 nm) and consistent across all the simulations. The same trend as observed earlier upon comparison of the simulations with the crystal structures was found: the structural differences were greater for domain II (rmsds of 0.52 ± 0.04 and 0.50 ± 0.09 nm with respect to PDB entries 1nql and 1yy9, respectively) than for domains I (rmsd of 0.20 ± 0.03 nm for both structures) and III (rmsd of 0.38 ± 0.06 nm for both structures). The fact that the comparison of the domains with the two inhibited structures yields similar rmsd values suggests that the differences between those structures and the structures of the sEGFR in the simulations are equivalent, regardless of the presence of the EGF or TGFα.

DISCUSSION

The communication and transmission of signals between the extracellular and cytosolic media are central to molecular physiology. The structure and function of membrane receptors such as the EGFR and the growth hormone receptor have long been a focus of intense interest: many studies have examined the binding of growth factors to the extracellular domains of their respective receptors, the kinetics of this process, and the effect on the receptor monomer–dimer equilibrium. Equally, work on the understanding of the interplay between the intracellular domains of the receptors, their various partners, and the subsequent activation of reaction cascades in the cytosol has been pursued. In contrast, a detailed understanding of the propagation of a signal across the plasma membrane has remained elusive.

Cytokine binding is not required for the formation of EGFR dimers but is necessary for activation.[17,19−21,47,48] Evidence from fluorescence spectroscopy and microscopy suggests that a significant proportion of the EGFR exists as preformed dimers on the cell surface.[21,33,49−51] A preformed unbound dimer has also been proposed for the *Drosophila melanogaster* EGFR.[52] In the simulations presented here, the apo dimer remained stable, despite the extensive motions of the domains between and within the protomers. In addition, the contact surface area of the dimerization interface remained unchanged (15 nm^2 on average), irrespective of the presence or absence of cytokine. Interestingly, the value of the interface area is close to those calculated by Kästner et al.[27] for the full-length extracellular domain of $(EGFR–EGF)_2$ in solution and bound to a lipid bilayer (approximately 12–14 and 15 nm^2, respectively). The absence of domain IV in the simulations does not seem to lead to an increase in the dimerization interface area. This is in contrast with an earlier simulation study of $(EGFR–EGF)_2$ in which it was proposed that the absence of domain IV would be compensated by an increased number of contacts between the two domains II.[28] Although the rmsd values calculated for domain II in the simulations of the apo dimer with respect to the starting crystal structures (0.56–0.63 nm) are larger than what is normally found for globular proteins, they are reasonable considering the size and nature of the receptor. Interestingly, domain II was also found to be the most flexible in simulations of the liganded and unliganded monomeric extracellular domain (rmsd of 0.3–0.6 nm).[29] Domain II is highly extended and consists of eight independent modules in an almost linear arrangement, but its flexibility had no effect on the dimerization interface area in all the simulations. Furthermore, no significant difference in the dimerization interface was observed between the 65 and 100 ns simulations of the unliganded EGFR. In particular, the association of the two dimerization arms (in module 5 in domains II) was maintained. This suggests that the interactions between the two modules 5 mediated by the dimerization arms contribute to the overall stability of the dimer. This is in agreement with experiments that showed that the stability of the dimer was significantly lower if the dimerization arms were deleted[21] and that the association of the dimerization arms was necessary for high-affinity binding of the EGF.[52] Figure 9 indicates that module 6 of domain II also contributes substantially to the dimerization interface in a cytokine binding-independent fashion. This is consistent with a study by Dawson et al.[13] that highlighted that mutations in modules 5 and 6 of domain II could abolish or impair receptor activation. The distances between the two domains III and IV in the simulations and the crystal structures were similar. This agrees with FRET (Förster resonance energy transfer) measurements of fluorescently labeled antibodies bound to the EGFR[50] that showed that the EGF-induced rotation of the transmembrane domain did not result in a significant change in the distance between the EGFR extracellular domains.

In the simulations, the removal of the EGF and TGFα from the sEGFR dimer caused a rearrangement within the dimer that involved a twist between the protomers (Figure 4). The magnitude of the twist depended on the crystal structure from which the apo dimer was derived. Specifically, the average rotation angle between the protomers was 64.7 ± 3.0° and 24.9 ± 8.7° in the apo sEGFR dimer derived from the EGF-bound ($sEGFR^E_2$) and TGFα-bound ($sEGFR^T_2$) dimers, respectively (Table 2). This difference could be related to the resolution of the starting crystal structures: 3.3 Å for $(sEGFR–EGF)_2$[8] and 2.5 Å for $(sEGFR–TGF\alpha)_2$.[10] There was also some limited rotation of the protomers in the simulations of the holo dimers, and the average effective twist angle between the protomers that can be attributed to the removal of the cytokines is 35.4° for $sEGFR^E_2$ and 16.3° for $sEGFR^T_2$. It is likely that the rotation observed in the liganded dimers is due to the removal of crystal packing forces. This is in line with a comparison of the structure of $(EGFR–EGF)_2$ from simulations in solution and in a crystal environment that showed that crystal packing effects led to a significant compaction of the dimer that constrained motions of the domains in the protomers.[28] Given that domain IV was not modeled in the simulations, the magnitude of the twist measured in the simulations may not be directly comparable to the results of experiments with full-length receptors. However, the relative rotation that occurred in the simulations is consistent with previous experiments with the untruncated EGFR that suggested that the activation of the EGFR dimer was associated with a twist of the two protomers. In a study by Moriki et al.,[17] a nonaalanine peptide was inserted in the juxtamembrane region in the EGFR and each single alanine was then mutated to a cysteine. From the propensity of each cysteine to cross-link the protomers in the presence and absence of EGF, it was concluded that binding of the ligand to the extracellular domain triggered a twist of the juxtamembrane regions in the plane parallel to the plasma membrane. Furthermore, fluorescence microscopy experiments also suggested that a relative rotational rearrangement of the protomers within the EGFR dimer was induced by the binding of the EGF.[33]

A model involving the relative rotation of the two protomers is reminiscent of the mechanism of activation proposed for the

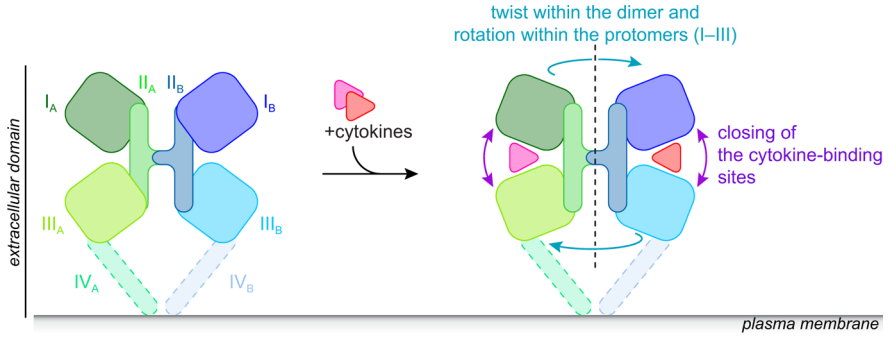

Figure 10. Schematic of the overall motions observed in the simulations of domains I–III of the homodimer of the EGFR extracellular domain. Motions involving domains IV (depicted with dashed lines) were not modeled.

growth hormone receptor (GHR) and the prolactin receptor (PRLR) that are also active as homodimers. In the case of GHR and PRLR, a relative rotation of the protomers was found in both experiment[53] and molecular dynamics simulations.[54,55] The latter revealed that the two extracellular domains underwent a relative rotation of approximately 45° for GHR and 20–30° for PRLR. GHR and PRLR are not RTKs but belong to the hematopoietin receptor family. The fact that the binding of a cytokine to receptors from different families causes a relative rotation between the two protomers suggests a general mechanism for receptor activation. However, unlike the activation of GHR and PRLR that entails rigid-body motions between individual protomers, the twist within the EGFR dimer arises from distortions within the protomers themselves. In all the simulations, the protomers experienced an internal twist about the long axis of domain II that consisted of a counterclockwise shift of domain I with respect to domains III. The motion in the two protomers occurred in a centrosymmetric fashion along the C_2 axis of the dimer (Figures 4 and 6). On average, the torsion angle was approximately 20°, 62°, and 39° in the liganded dimers, $sEGFR^E_2$, and $sEGFR^T_2$, respectively (Table 2). This twisting motion was previously suggested by a principal component analysis of the dominant motion in a 12 ns simulation of $(sEGFR–EGF)_2$.[28] Liu et al.[56] described the conformation of the crystal structure of $(sEGFR–EGF)_2$ as "staggered" and less stable than the "flush" arrangement in the crystal structure of $(sEGFR–TGF\alpha)_2$, which consists of the domains facing each other in register. Our simulations would suggest otherwise. In the absence of crystal packing effects, both the apo and holo dimers relaxed to a more staggered arrangement (the magnitude of the motion being greater in the absence of bound cytokines). This contrasts with the study of $(EGFR–EGF)_2$ by Arkhipov et al.[31] that reported that the ligand-free dimer adopted a flush arrangement after simulation for 11 μs. Note that their model included domain IV that bent to such an extent that the C-terminus of domain IV in one protomer was projected toward the hinge region connecting domains III and IV in the other protomer. This orientation appears to be incompatible with domain IV linking the extracellular domain to a transmembrane domain and would suggest that the presence of domain IV in the absence of a membrane may have a substantial effect on the relative orientation of the protomers in the unliganded state. Various staggered and flush orientations between the protomers were also found in liganded EGFR homodimers where other growth factors (amphiregulin, betacellulin, epigen, epiregulin, and heparin-binding EGF-like growth factor) had been docked into the cytokine-binding sites and then allowed to relax.[30]

In the simulations, a consequence of the twist within the protomers was a change in the configuration of the ligand-binding sites. In the simulations of $sEGFR^E_2$, the ligand-binding sites became more open ($\theta \approx 74°$) than the crystal structure ($\theta \approx 56°$), whereas it was unchanged in three of the four simulations of $sEGFR^T_2$ ($\theta \approx 55°$). In the fourth simulation of $sEGFR^T_2$, the opening of the ligand-binding sites was similar to that observed with $sEGFR^E_2$. This suggests that the closed state is metastable on the time scale of the simulations and that the differences observed are related to differences in the precision of the starting models (that is the crystal structures).

Despite the twists between and within the protomers, the internal structure of each domain was retained in all the simulations irrespective of the presence of a cytokine. The superimposition of the final structures of the domains from all the simulations gave rmsd values lower than those of the crystal structures, indicating a degree of convergence in the simulations regardless of the presence of a cytokine. The rmsds calculated for the whole protomers and the individual domains also compare favorably with rmsds calculated in previous simulation studies of $(EGFR–EGF)_2$ in solution or in the presence of a membrane.[27,28] More importantly, the comparison of the structures of the domains in the simulations with those found in the tethered structures of the extracellular domain of the EGFR[23,24] showed that there was little difference among the inhibited, unliganded, and cytokine-bound states of the EGFR. Therefore, the activation of the EGFR and the inherent relative rotation between and within the two protomers observed in the simulations appear to be due to rigid-body motions of the individual domains, preserving the global structure of the dimer. The rigidity of the domains was previously suggested in simulations of $(EGFR–EGFR)_2$ in water and in the presence of a model membrane (the receptor included domain IV),[27] suggesting that the environment, the relative orientation of the extracellular domain with respect to a membrane, and its overall structure have no or little effect on the structure of domains I–III. Motions primarily took place in the plane parallel to the surface of the plasma membrane. No stretching, compression, or relative translation of the protomers along the dimerization axis was observed during the simulations. This is in line with experimental cross-linking studies in which cysteine residues were added in the extracellular juxtamembrane region.[17] The fact that disulifde bonds between the protomers can form requires that the two cysteines be at the same position with respect to the plane of

dx.doi.org/10.1021/bi401632z | *Biochemistry* 2014, 53, 2710–2721

the plasma membrane. A cartoon of the proposed motions is shown in Figure 10.

In summary, the molecular dynamics simulations in this study suggest that a relative rotation between the two protomers occurs upon binding of cytokines to the EGFR homodimer. The change in the relative orientation between the protomers was associated with internal rearrangements within the protomers and resulted in a staggered arrangement of domains I and III along the axis defined by domain II. Although the simulated extracellular domain did not include domains IV, the simulations provide a detailed description of the motions and structural changes involved between the domains within each protomer.

AUTHOR INFORMATION

Corresponding Author

*E-mail: d.poger@uq.edu.au. Phone: +61 (0)7 3365 7562. Fax: +61 (0)7 3365 3872.

Funding

This work was funded by the Australian Research Council (Projects DP110100327, DP130102153, and LE120100181).

Notes

The authors declare no competing financial interest.

ACKNOWLEDGMENTS

This work was supported by high-performance computational resources on the National Computational Infrastructure (NCI) National Facility and iVEC located at iVEC@Murdoch through the National Computational Merit Allocation Scheme (Project m39).

ABBREVIATIONS

EGF, epidermal growth factor; EGFR, epidermal growth factor receptor; rmsd, root-mean-square deviation; sEGFR, soluble epidermal growth factor receptor; TGFα, transforming growth factor α.

REFERENCES

(1) Heldin, C.-K. (1995) Dimerization of cell surface receptors in signal transduction. *Cell 80*, 213−223.

(2) Jiang, Q., and Hunter, T. (1999) Receptor signaling: When dimerization is not enough. *Curr. Biol. 9*, R568−R571.

(3) Schlessinger, J. (2000) Cell signaling by receptor tyrosine kinases. *Cell 103*, 211−225.

(4) Yarden, Y., and Sliwkowski, M. X. (2001) Untangling the ErbB signalling network. *Nat. Rev. Mol. Cell Biol. 2*, 127−137.

(5) Sergina, N. V., and Moasser, M. M. (2007) The HER family and cancer: Emerging molecular mechanisms and therapeutic targets. *Trends Mol. Med. 13*, 527−534.

(6) Sibilia, M., Kroismayr, R., Lichtenberger, B. M., Natarajan, A., Hecking, M., and Holcmann, M. (2007) The epidermal growth factor receptor: From development to tumorigenesis. *Differentiation 75*, 770−787.

(7) Roskoski, R., Jr. (2014) The ErbB/HER family of protein-tyrosine kinases and cancer. *Pharmacol. Res. 79*, 34−74.

(8) Ogiso, H., Ishitani, R., Nureki, O., Fukai, S., Yamanaka, M., Kim, J.-H., Saito, K., Sakamoto, A., Inoue, M., Shirouzu, M., and Yokoyama, S. (2002) Crystal structure of the complex of human epidermal growth factor and receptor extracellular domains. *Cell 110*, 775−787.

(9) Lu, C., Mi, L.-Z., Grey, M. J., Zhu, J., Graef, E., Yokoyama, S., and Springer, T. A. (2010) Structural evidence for loose linkage between ligand binding and kinase activation in the epidermal growth factor receptor. *Mol. Cell. Biol. 30*, 5432−5443.

(10) Garrett, T. P. J., McKern, N. M., Lou, M., Elleman, T. C., Adams, T. E., Lovrecz, G. O., Zhu, H.-J., Walker, F., Frenkel, M. J., Hoyne, P. A., Jorissen, R. N., Nice, E. C., Burgess, A. W., and Ward, C. W. (2002) Crystal structure of a truncated epidermal growth factor receptor extracellular domain bound to transforming growth factor α. *Cell 110*, 763−773.

(11) Bajaj, M., Waterfield, M. D., Schlessinger, J., Taylor, W. R., and Blundell, T. (1987) On the tertiary structure of the extracellular domains of the epidermal growth factor and insulin receptors. *Biochim. Biophys. Acta 916*, 220−226.

(12) Ward, C. W., Hoyne, P. A., and Flegg, R. H. (1995) Insulin and epidermal growth factor receptors contain the cysteine repeat motif found in the tumor necrosis factor receptor. *Proteins: Struct., Funct., Bioinf. 22*, 141−153.

(13) Dawson, J. P., Berger, M. B., Lin, C. C., Schlessinger, J., Lemmon, M. A., and Ferguson, K. M. (2005) Epidermal growth factor receptor dimerization and activation require ligand-induced conformational changes in the dimer interface. *Mol. Cell. Biol. 25*, 7734−7742.

(14) Schlessinger, J., Plotnikov, A. N., Ibrahimi, O. A., Eliseenkova, A. V., Yeh, B. K., Yayon, A., Linhardt, R. J., and Mohammadi, M. (2000) Crystal structure of a ternary FGF-FGFR-heparin complex reveals a dual role for heparin in FGFR binding and dimerization. *Mol. Cell 6*, 743−750.

(15) Liu, H., Chen, X., Focia, P. J., and He, X. (2007) Structural basis for stem cell factor-KIT signaling and activation of class III receptor tyrosine kinases. *EMBO J. 26*, 891−901.

(16) Yuzawa, S., Opatowsky, Y., Zhang, Z., Mandiyan, V., Lax, I., and Schlessinger, J. (2007) Structural basis for activation of the receptor tyrosine kinase KIT by stem cell factors. *Cell 130*, 323−334.

(17) Moriki, T., Maruyama, H., and Maruyama, I. N. (2001) Activation of preformed EGF receptor dimers by ligand-induced rotation of the transmembrane domain. *J. Mol. Biol. 311*, 1011−1026.

(18) Yu, X., Sharma, K. D., Takahashi, T., Iwamoto, R., and Mekada, E. (2002) Ligand-independent dimer formation of epidermal growth factor receptor (EGFR) is a step separable from ligand-induced EGFR signaling. *Mol. Biol. Cell 13*, 2547−2557.

(19) Clayton, A. H., Walker, F., Orchard, S. G., Henderson, C., Fuchs, D., Rothacker, J., Nice, E. C., and Burgess, A. W. (2005) Ligand-induced dimer-tetramer transition during the activation of the cell surface epidermal growth factor receptor: A multidimensional microscopy analysis. *J. Biol. Chem. 280*, 30392−30399.

(20) Tao, R.-H., and Maruyama, I. N. (2008) All EGF(ErbB) receptors have preformed homo- and heterodimeric structures in living cells. *J. Cell Sci. 121*, 3207−3217.

(21) Chung, I., Akita, R., Vandlen, R., Toomre, D., Schlessinger, J., and Mellman, I. (2010) Spatial control of EGF receptor activation by reversible dimerization on living cells. *Nature 464*, 783−787.

(22) Walker, F., Rothacker, J., Henderson, C., Nice, E. C., Catimel, B., Zhang, H.-H., Scott, A. M., Bailey, M. F., Orchard, S. G., Adams, T. E., Liu, Z., Garrett, T. P., Clayton, A. H. A., and Burgess, A. W. (2012) Ligand binding induces a conformational change in epidermal growth factor receptor dimers. *Growth Factors 30*, 394−409.

(23) Ferguson, K. M., Berger, M. B., Mendrola, J. M., Cho, H.-S., Leahy, D. J., and Lemmon, M. A. (2003) EGF activates its receptor by removing interactions that autoinhibit ectodomain dimerization. *Mol. Cell 11*, 507−517.

(24) Li, S., Schmitz, K. R., Jeffrey, P. D., Wiltzius, J. J. W., Kussie, P., and Ferguson, K. M. (2005) Structural basis for inhibition of the epidermal growth factor receptor by cetuximab. *Cancer Cell 7*, 301−311.

(25) Burgess, A. W., Cho, H.-S., Eigenbrot, C., Ferguson, K. M., Garrett, T. P. J., Leahy, D. J., Lemmon, M. A., Sliwkowski, M. X., Ward, C. W., and Yokoyama, S. (2003) An open-and-shut case? Recent insights into the activation of EGF/ErbB receptors. *Mol. Cell 12*, 541−552.

(26) Dawson, J. P., Bu, Z., and Lemmon, M. A. (2007) Ligand-induced structural transitions in ErbB receptor extracellular domains. *Structure 15*, 942−954.

(27) Kästner, J., Loeffler, H. H., Roberts, S. K., Martin-Fernandez, M., and Winn, M. D. (2009) Ectodomain orientation, conformational plasticity and oligomerization of ErbB1 receptors investigated by molecular dynamics. *J. Struct. Biol. 167*, 117−128.
(28) Zhang, Z., and Wriggers, W. (2011) Polymorphism of the epidermal growth factor receptor extracellular ligand binding domain: The dimer interface depends on domain stabilization. *Biochemistry 50*, 2144−2156.
(29) Loeffler, H. H., and Winn, M. D. (2013) Ligand binding and dynamics of the monomeric epidermal growth factor receptor ectodomain. *Proteins: Struct., Funct., Bioinf. 81*, 1931−1943.
(30) Sanders, J. M., Wampole, A. E., Thakur, M. L., and Wickstrom, E. (2013) Molecular determinants of epidermal growth factor binding: A molecular dynamics study. *PLoS One 8*, e54136.
(31) Arkhipov, A., Shan, Y., Das, R., Endres, N. F., Eastwood, M. P., Wemmer, D. E., Kuriyan, J., and Shaw, D. E. (2013) Architecture and membrane interactions of the EGF receptor. *Cell 152*, 557−569.
(32) Endres, N. F., Das, R., Smith, A. W., Arkhipov, A., Kovacs, E., Huang, Y., Pelton, J. G., Shan, Y., Shaw, D. E., Wemmer, D. E., Groves, J. T., and Kuriyan, J. (2013) Conformational coupling across the plasma membrane in activation of the EGF receptor. *Cell 152*, 543−556.
(33) Gadella, T. W., Jr., and Jovin, T. M. (1995) Oligomerization of epidermal growth factor receptors on A431 cells studied by time-resolved fluorescence imaging microscopy. A stereochemical model for tyrosine kinase receptor activation. *J. Cell Biol. 129*, 1543−1558.
(34) DeLano, W. L. (2002) *The PyMOL Molecular Graphics System*, DeLano Scientific, San Carlos, CA.
(35) van der Spoel, D., Lindahl, E., Hess, B., Groenhof, G., Mark, A. E., and Berendsen, H. J. C. (2005) GROMACS: Fast, flexible, and free. *J. Comput. Chem. 26*, 1701−1718.
(36) Schmid, N., Eichenberger, A. P., Choutko, A., Riniker, S., Winger, M., Mark, A. E., and van Gunsteren, W. F. (2011) Definition and testing of the GROMOS force-field versions 54a7 and 54b7. *Eur. Biophys. J. 40*, 843−856.
(37) Berendsen, H. J. C., Postma, J. P. M., van Gunsteren, W. F., DiNola, A., and Haak, J. R. (1984) Molecular dynamics with coupling to an external bath. *J. Chem. Phys. 81*, 3684−3690.
(38) Hess, B., Bekker, H., Berendsen, H. J. C., and Fraaije, J. G. E. M. (1997) Lincs: A linear constraint solver for molecular simulations. *J. Comput. Chem. 18*, 1463−1472.
(39) Berendsen, H. J. C., Postma, J. P. M., van Gunsteren, W. F., and Hermans, J. (1981) Interaction models for water in relation to protein hydration. In *Intermolecular Forces* (Pullman, B., Ed.) pp 331−342, Reidel, Dordrecht, The Netherlands.
(40) Miyamoto, S., and Kollman, P. A. (1992) Settle: An analytical version of the shake and rattle algorithm for rigid water models. *J. Comput. Chem. 13*, 952−962.
(41) Feenstra, K., Hess, B., and Berendsen, H. J. C. (1999) Improving efficiency of large time-scale molecular dynamics simulations of hydrogen-rich systems. *J. Comput. Chem. 20*, 786−798.
(42) Tironi, I. G., Sperb, R., Smith, P. E., and van Gunsteren, W. F. (1995) A generalized reaction field method for molecular dynamics simulations. *J. Chem. Phys. 102*, 5451−5459.
(43) Heinz, T. N., van Gunsteren, W. F., and Hünenberger, P. H. (2001) Comparison of four methods to compute the dielectric permittivity of liquids from molecular dynamics simulations. *J. Chem. Phys. 115*, 1125−1136.
(44) Lee, B., and Richards, F. M. (1971) The interpretation of protein structures: Estimation of static accessibility. *J. Mol. Biol. 55*, 379−400.
(45) Varshney, A., Brooks, F. P., Jr., and Wright, W. V. (1994) Computing smooth molecular surfaces. *IEEE Computer Graphics and Applications 14*, 19−25.
(46) Humphrey, W., Dalke, A., and Schulten, K. (1996) VMD: Visual molecular dynamics. *J. Mol. Graphics 14*, 33−38.
(47) Ichinose, J., Murata, M., Yanagida, T., and Sako, Y. (2004) EGF signalling amplification induced by dynamic clustering of EGFR. *Biochem. Biophys. Res. Commun. 324*, 1143−1149.
(48) Clayton, A. H., Orchard, S. G., Nice, E. C., Posner, R. G., and Burgess, A. W. (2008) Predominance of activated EGFR higher-order oligomers on the cell surface. *Growth Factors 26*, 316−324.
(49) Bader, A. N., Hofman, J., abd Voortman, E. G., van Bergen en Henegouwen, P. M. P., and Gerritsen, H. C. (2009) Homo-FRET imaging enables quantification of protein cluster sizes with subcellular resolution. *Biophys. J. 97*, 2613−2622.
(50) Martin-Fernandez, M., Clarke, D. T., Tobin, M. J., Jones, S. V., and Jones, G. R. (2002) Preformed oligomeric epidermal growth factor receptors undergo an ectodomain structure change during signaling. *Biophys. J. 82*, 2415−2427.
(51) Szabó, A., Horváth, G., Szöllösi, J., and Nagy, P. (2008) Quantitative characterization of the large-scale association of ErbB1 and ErbB2 by flow cytometric homo-FRET measurements. *Biophys. J. 95*, 2086−2096.
(52) Alvarado, D., Klein, D. E., and Lemmon, M. A. (2010) Structural basis for negative cooperativity in growth factor binding to an EGF receptor. *Cell 142*, 568−579.
(53) Brown, R. J., Adams, J. J., Pelekanos, R. A., Wan, Y., McKinstry, W. J., Palethorpe, K., Seeber, R. M., Monks, T. A., Eidne, K. A., Parker, M. W., and Waters, M. J. (2005) Model for growth hormone receptor activation based on subunit rotation within a receptor dimer. *Nat. Struct. Mol. Biol. 12*, 814−821.
(54) Groothuizen, F. S., Poger, D., and Mark, A. E. (2010) Activating the prolactin receptor: Effect of the ligand on the conformation of the extracellular domain. *J. Chem. Theory Comput. 6*, 3274−3283.
(55) Poger, D., and Mark, A. E. (2010) Turning the growth hormone receptor on: Evidence that hormone binding induces subunit rotation. *Proteins: Struct., Funct., Bioinf. 78*, 1163−1174.
(56) Liu, P., Cleveland, T. E., IV, Bouyain, S., Byrne, P. O., Longo, P. A., and Leahy, D. J. (2012) A single ligand is sufficient to activate EGFR dimers. *Proc. Natl. Acad. Sci. U.S.A. 109*, 10861−10866.